

Mean field effects on the scattered atoms in condensate collisions

P. Deuar¹, P. Ziń², J. Chwedeńczuk³, and M. Trippenbach^{3,a}

¹ Institute of Physics, Polish Academy of Sciences, Al. Lotników 32/46, 02-668 Warsaw, Poland

² The Andrzej Sołtan Institute for Nuclear Studies, Hoża 69, 00-681 Warsaw, Poland

³ Institute of Theoretical Physics, Physics Department, University of Warsaw, Hoża 69, 00-681 Warsaw, Poland

Received 28 January 2011 / Received in final form 6 May 2011

Published online 28 June 2011 – © EDP Sciences, Società Italiana di Fisica, Springer-Verlag 2011

Abstract. We consider the collision of two Bose Einstein condensates at supersonic velocities and focus on the halo of scattered atoms. This halo is the most important feature for experiments and is also an excellent testing ground for various theoretical approaches. In this study we find that the typical reduced Bogoliubov description, commonly used, is often not accurate in the region of parameters where experiments are performed. Surprisingly, besides the halo pair creation terms, one should take into account the evolving mean field of the remaining condensate and on-condensate pair creation. We present examples where the difference is clearly seen, and where the reduced description still holds. We also demonstrate how to investigate separately the effects of various physical processes that influence the properties of the halo.

1 Introduction

When two Bose-Einstein condensates (BECs) collide at sufficiently high velocity, pairs of atoms are scattered out of the condensates. After many scattering events, a distinct halo of atom pairs is formed in momentum space. This was observed in many experiments [1–17] and analyzed in numerous theoretical works [1,7,11,18–34]. The formation of a halo starts spontaneously and is analogous to the generation of photon pairs in parametric down conversion. Such photon pairs were used to observe Bell inequality violation [35], and can be applied for quantum cryptography [36] or quantum teleportation [37]. In analogy, atoms formed in the collision of two BECs have a potential application for precision measurements [38], interferometry [2,39–42], or tests of quantum mechanics [43].

The simplest model that captures the formation of a halo in the condensate collision is the “reduced Bogoliubov” model (RBM), used by many authors [17–22,25,26,28,31,32]. In this formulation, the two condensates counter-propagate at a constant relative velocity and without change of shape. The wave-packets enter in the Bogoliubov equation for the field of scattered atoms as a classical source. The RBM can be used to calculate various observables, such as the density of scattered atoms or their second-order correlation functions, which can be directly compared with the experimental data. The predictions of the RBM are often in good agreement with experiment [31], but there are cases where more complete models have shown significant departures from the RBM [1,29,32].

Here we carry out the first systematic analysis of the effect of the terms that are neglected in the RBM. Surprisingly, it turns out that they can be very important, and can qualitatively change the behaviour of the halo, as well as the number of scattered particles by a factor of several. This is the major conclusion of the paper. We also show how the stochastic method used is a convenient tool for taking apart the evolution of the system piece by piece to identify the effect of the various physical processes.

The paper is organised as follows. In Section 2 we introduce both the RBM and full Bogoliubov models and the numerical method of solving the equations of motion. Two additional simplified formulations, also introduced in Section 2, are used to investigate the properties of the halo. The dependence of the halo shape on the model is shown in Section 3.1 for two characteristic cases, whereas Section 3.2 explains in detail the dependence of the halo position on the degree of simplifications made. We also indicate the range of interaction strength for which the RBM is quantitatively accurate.

2 Bogoliubov approach to the scattering of atoms in a BEC collision

2.1 Scattering in condensate collisions

Initially the gas is trapped by a harmonic potential. In order to start the (half-) collision, a superposition of two counter-propagating, mutually coherent, atomic clouds of equal density is prepared by shining a Bragg pulse. The trap is simultaneously turned off. The two fractions move

^a e-mail: marek.trippenbach@fuw.edu.pl

apart with relative speed $2v_{\text{rec}}$ along the z axis, where v_{rec} is the atomic recoil velocity. If the relative velocity is larger than the speed of sound at the condensate center, the collision is supersonic, superfluidity breaks down and a halo of scattered atoms is formed. The physical properties of this halo are the main subject of this study.

In our approach we model the process of the halo formation using a time dependent Bogoliubov method, where the field operator is defined as

$$\hat{\Psi}(\mathbf{x}, t) = \phi(\mathbf{x}, t) + \hat{\delta}(\mathbf{x}, t). \quad (1)$$

Here, $\phi(\mathbf{x}, t)$ is the condensate wave function governed by the GP equation

$$i\hbar\partial_t\phi(\mathbf{x}, t) = \left(-\frac{\hbar^2}{2m}\nabla^2 + g|\phi(\mathbf{x}, t)|^2\right)\phi(\mathbf{x}, t). \quad (2)$$

It is normalized to N – the number of atoms in the condensate, which remains undepleted during the dynamics. The coupling constant g relates to the scattering length a through $g = 4\pi\hbar^2 a/m$, where m is a mass of an atom. The field operator $\hat{\delta}(\mathbf{x}, t)$ describes the non-condensed atoms (both the quantum depletion and the scattered halo) and satisfies the following equation

$$i\hbar\partial_t\hat{\delta}(\mathbf{x}, t) = \left(-\frac{\hbar^2}{2m}\nabla^2 + 2g|\phi(\mathbf{x}, t)|^2\right)\hat{\delta}(\mathbf{x}, t) + g\phi^2(\mathbf{x}, t)\hat{\delta}^\dagger(\mathbf{x}, t). \quad (3)$$

From this equation, we can trace back an effective Bogoliubov Hamiltonian:

$$\hat{H}_{\text{eff}} = \int d^3\mathbf{x} \hat{\delta}^\dagger(\mathbf{x}) \left(-\frac{\hbar^2}{2m}\nabla^2\right) \hat{\delta}(\mathbf{x}) \quad (4a)$$

$$+ 2g \int d^3\mathbf{x} |\phi(\mathbf{x})|^2 \hat{\delta}^\dagger(\mathbf{x}) \hat{\delta}(\mathbf{x}) \quad (4b)$$

$$+ \frac{g}{2} \int d^3\mathbf{x} \phi^2(\mathbf{x}) \hat{\delta}^\dagger(\mathbf{x}) \hat{\delta}^\dagger(\mathbf{x}) + h.c. \quad (4c)$$

Line (4a) stands for kinetic energy, while line (4b) results from the interaction of the condensate mean-field with the scattered atoms. Finally (4c) describes the creation/annihilation process of pairs of non-condensed atoms.

Most salient features of BEC collisions are already found for the case of initially spherically symmetric condensates. Before the numerical simulation of the collision, we find the condensate wave-function as a ground state of the Gross-Pitaevskii equation with harmonic trap of frequency ω ,

$$\mu\phi_0(\mathbf{x}) = \left(-\frac{\hbar^2}{2m}\nabla^2 + \frac{1}{2}m\omega^2\mathbf{x}^2 + g|\phi_0(\mathbf{x})|^2\right)\phi_0(\mathbf{x}). \quad (5)$$

Next, the trap is turned off and at the same time a set of Bragg pulses is applied [14]. In the center-of-mass frame, the initial state is then

$$\phi(\mathbf{x}, 0) = A\phi_0(\mathbf{x}) (e^{ik_0z} + e^{-ik_0z}), \quad (6)$$

where A is the normalization constant and $k_0 = mv_{\text{rec}}/\hbar$ is the wave-vector associated with the recoil velocity. The initial state of the non-condensed part is taken to be a vacuum

$$\hat{\delta}(\mathbf{x}, 0)|0\rangle = 0. \quad (7)$$

From this initial state the system evolves according to equations (2) and (3).

2.2 Dimensionless parameters

We point out that in our approximate description (Bogoliubov method), there is a universal scaling such that the non-condensed field $\hat{\delta}(\mathbf{x})$ is identical in all systems having the same value of gN (or aN , where a is a scattering length). Hence the dynamics is described by the length scale aN rather than by the scattering length a or the number of particles N separately. Other important length scales are $a_{ho} = \sqrt{\hbar/m\omega}$ – the harmonic oscillator length, and $1/k_0$. Alternatively, since there is no trap for $t > 0$, we can use the width of the initial condensate σ instead of a_{ho} . If we apply the Thomas-Fermi approximation [44], a good choice of characteristic width σ is the Thomas Fermi radius $R_{TF} = (15Ng/4\pi m\omega^2)^{1/5}$. In conclusion: there are three relevant length scales, hence our system can be characterized by two dimensionless parameters. We choose: $\beta = k_0\sigma$ and $\alpha = aN/\sigma$ (see [25,26,28,31]).

The first parameter β is independent of interactions and has a kinetic character. It can be viewed as the number of fringes created by the Bragg pulses on the initial condensate, or as a ratio of the dispersion time scale, $m\sigma^2/\hbar$ to the collision timescale, $(m\sigma)/(\hbar k_0)$, see for instance [25,26,28,31]. In realistic situations $\beta \gg 1$.

The second parameter α is proportional to the ratio of the interaction energy per particle gN/σ^3 to the kinetic energy per particle in the initial condensate $\hbar^2/(2m\sigma^2)$. It is related to $\alpha^{(\text{past})} = mgN/(\sigma\hbar^2\pi^{3/2})$ which has been used previously [25,26,28,31], but differs by a numerical factor: $\alpha = (\sqrt{\pi}/4)\alpha^{(\text{past})}$. The ratio between α and β quantifies the strength and nature of scattering. It has been shown that Bose enhancement of scattering occurs for $\alpha \gtrsim \beta$ [26].

2.3 Simulation of dynamics using a positive-P Bogoliubov method

The positive-P representation can be used to fully represent the Bogoliubov field $\hat{\delta}$ as an ensemble of complex stochastic variable fields $\psi(\mathbf{x}, t)$ and $\tilde{\psi}(\mathbf{x}, t)$. The dynamics of the system (3) can then be shown by standard phase-space methods [45–48] to be equivalent to stochastic Langevin equations which take the following form in the Ito calculus:

$$i\hbar\partial_t\psi(\mathbf{x}, t) = \left(-\frac{\hbar^2}{2m}\nabla^2 + 2g|\phi(\mathbf{x}, t)|^2\right)\psi(\mathbf{x}, t) + g\phi(\mathbf{x}, t)^2\tilde{\psi}(\mathbf{x}, t)^* + \sqrt{i\hbar g}\phi(\mathbf{x}, t)\xi(\mathbf{x}, t), \quad (8a)$$

$$i\hbar\partial_t\tilde{\psi}(\mathbf{x}, t) = \left(-\frac{\hbar^2}{2m}\nabla^2 + 2g|\phi(\mathbf{x}, t)|^2\right)\tilde{\psi}(\mathbf{x}, t) + g\phi(\mathbf{x}, t)^2\psi(\mathbf{x}, t)^* + \sqrt{i\hbar g}\phi(\mathbf{x}, t)\tilde{\xi}(\mathbf{x}, t). \quad (8b)$$

Here $\xi(\mathbf{x}, t)$ and $\tilde{\xi}(\mathbf{x}, t)$ are delta-correlated, independent, real stochastic noise fields with zero mean. The second moments are equal to

$$\begin{aligned}\langle \xi(\mathbf{x}, t) \tilde{\xi}(\mathbf{x}', t') \rangle &= 0 \quad \text{and} \\ \langle \xi(\mathbf{x}, t) \xi(\mathbf{x}', t') \rangle &= \langle \tilde{\xi}(\mathbf{x}, t) \tilde{\xi}(\mathbf{x}', t') \rangle \\ &= \delta(\mathbf{x} - \mathbf{x}') \delta(t - t').\end{aligned}$$

Numerically, ξ and $\tilde{\xi}$ are approximated by real Gaussian random variables of variance $1/(\Delta t \Delta V)$ that are independent at each point at the computational lattice (of volume ΔV), and at each time step of length Δt .

Note that in the Stratonovich calculus, additional correction terms occur. The precise derivation of the stochastic Bogoliubov method presented above has been given in [49]. It has been previously used to simulate BEC collisions [1,2].

Any physical quantity is obtained by substituting $\hat{\delta}^\dagger \rightarrow \tilde{\psi}^*$ and $\hat{\delta} \rightarrow \psi$ and changing from a quantum average of the normally-ordered operator to a stochastic average [50],

$$\left\langle \prod_j \hat{\delta}^\dagger(\mathbf{x}_j) \prod_k \hat{\delta}(\mathbf{x}_k) \right\rangle = \lim_{m_r \rightarrow \infty} \left\langle \prod_{j,k} \tilde{\psi}(\mathbf{x}_j)^* \psi(\mathbf{x}_k) \right\rangle_{st}.$$

The braces $\langle \cdot \rangle_{st}$ denote the statistical average over m_r realizations. Observables in k -space follow from the Fourier transformation. For example, the one-particle density reads

$$\rho_1(\mathbf{k}, \mathbf{k}') = \phi(\mathbf{k})^* \phi(\mathbf{k}') + \text{Re} \langle \tilde{\psi}(\mathbf{k})^* \psi(\mathbf{k}') \rangle_{st}.$$

The stochastic equations (8) strictly reproduce the full quantum dynamics described by \hat{H}_{eff} when the number of samples tends to infinity. For finite sample sizes, one obtains an estimator for the full quantum dynamics, with an uncertainty that is calculated by standard methods [48].

2.4 Partially reduced Bogoliubov models

A fortuitous “side-effect” of the method formulated above is the possibility to systematically add or remove parts of the effective Hamiltonian (4) and GP equation (2) to understand their impact on the dynamics of the $\hat{\delta}$ field. This includes a numerical simulation of the RBM. To do this, we first write the condensate wavefunction as a sum of left- and right-moving wavepackets,

$$\phi(\mathbf{x}, t) = \phi_L(\mathbf{x}, t) + \phi_R(\mathbf{x}, t), \quad (9)$$

where $\phi_{L/R}(\mathbf{x}, 0) \propto \phi_0(\mathbf{x}) e^{\pm i k_0 z}$ with the GP equation

$$i\hbar \partial_t \phi_{L/R}(\mathbf{x}, t) = \left(-\frac{\hbar^2}{2m} \nabla^2 \right. \quad (10a)$$

$$+ g |\phi_{L/R}(\mathbf{x}, t)|^2 \quad (10b)$$

$$+ 2g |\phi_{R/L}(\mathbf{x}, t)|^2 \quad (10c)$$

$$\left. + g \phi_{R/L}(\mathbf{x}, t)^* \phi_{L/R}(\mathbf{x}, t) \right) \quad (10d)$$

$$\times \phi_{L/R}(\mathbf{x}, t).$$

The terms proportional to the coupling constant g can be interpreted as the self-interaction of the wavepacket (10b) and cross-interaction between different wavepackets (10c) respectively. The remaining terms are in line (10d).

Next, the decomposition (9) is put into the Bogoliubov Hamiltonian (4) giving

$$\hat{H}_{\text{eff}} = \int d^3 \mathbf{x} \hat{\delta}^\dagger(\mathbf{x}) \left(-\frac{\hbar^2}{2m} \nabla^2 \right) \hat{\delta}(\mathbf{x}) \quad (11a)$$

$$+ 2g \int d^3 \mathbf{x} |\phi_L(\mathbf{x}) + \phi_R(\mathbf{x})|^2 \hat{\delta}^\dagger(\mathbf{x}) \hat{\delta}(\mathbf{x}) \quad (11b)$$

$$+ g \int d^3 \mathbf{x} \phi_L(\mathbf{x}) \phi_R(\mathbf{x}) \hat{\delta}^\dagger(\mathbf{x}) \hat{\delta}^\dagger(\mathbf{x}) + h.c. \quad (11c)$$

$$+ \frac{g}{2} \int d^3 \mathbf{x} (\phi_L(\mathbf{x})^2 + \phi_R(\mathbf{x})^2) \hat{\delta}^\dagger(\mathbf{x}) \hat{\delta}^\dagger(\mathbf{x}) + h.c. \quad (11d)$$

The resonant term (11c) governs the process where two atoms, one from $\phi_R(\mathbf{x})$ and one from $\phi_L(\mathbf{x})$, collide and elastically scatter into the halo localized around the radius $|\mathbf{k}| \approx k_0$ as in the usual RBM. The line (11d) leads to creation of two atoms in the $\hat{\delta}$ field originating from one wave-packet, and we call this here “off-resonant pairing”. This includes quantum depletion processes.

Note that the specific form of equations (10)–(11) allows for removal of chosen terms. This way, one can inspect their role in the dynamics of the system. For instance, we can neglect all terms but the kinetic energy (11a) and pair production (11c) in the Bogoliubov Hamiltonian. This simplification we call the pair production (PP) dynamics. Within this approximation, the positive P formulation takes the form:

$$\begin{aligned}i\hbar \partial_t \psi(\mathbf{x}, t) &= -\frac{\hbar^2 \nabla^2}{2m} \psi(\mathbf{x}, t) \\ &+ 2g \phi_L(\mathbf{x}, t) \phi_R(\mathbf{x}, t) \tilde{\psi}(\mathbf{x}, t)^* \\ &+ \sqrt{2i\hbar g \phi_L(\mathbf{x}, t) \phi_R(\mathbf{x}, t)} \xi(\mathbf{x}, t), \quad (12a)\end{aligned}$$

$$\begin{aligned}i\hbar \partial_t \tilde{\psi}(\mathbf{x}, t) &= -\frac{\hbar^2 \nabla^2}{2m} \tilde{\psi}(\mathbf{x}, t) \\ &+ 2g \phi_L(\mathbf{x}, t) \phi_R(\mathbf{x}, t) \psi(\mathbf{x}, t)^* \\ &+ \sqrt{2i\hbar g \phi_L(\mathbf{x}, t) \phi_R(\mathbf{x}, t)} \tilde{\xi}(\mathbf{x}, t). \quad (12b)\end{aligned}$$

We can also simplify the GP equation (11) neglecting all the nonlinear terms and approximating the kinetic energy operator. As a result of this treatment we obtain the stiff movement (SM) of the counter-propagating wave-packets,

$$i\hbar \partial_t \phi_L(\mathbf{x}, t) = -\frac{\hbar^2 k_0}{2m} \left(k_0 - 2i \frac{\partial}{\partial z} \right) \phi_L(\mathbf{x}, t), \quad (13a)$$

$$i\hbar \partial_t \phi_R(\mathbf{x}, t) = -\frac{\hbar^2 k_0}{2m} \left(k_0 + 2i \frac{\partial}{\partial z} \right) \phi_R(\mathbf{x}, t). \quad (13b)$$

The RBM, described in literature, consists of both the PP (pair production) and SM (stiff movement) simplifications. Also, using alternative combinations of the approximations described above, we can generate four different

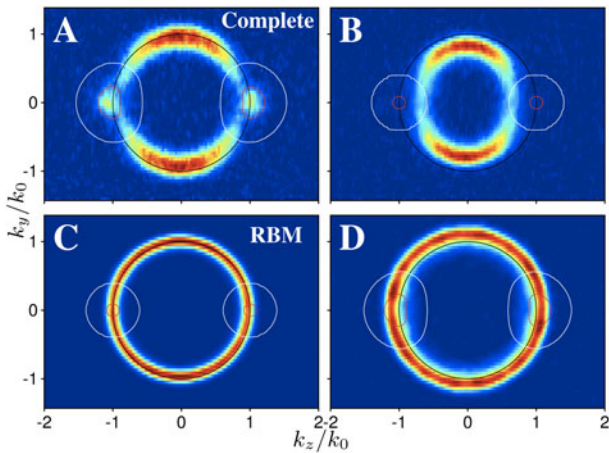


Fig. 1. (Color online) Cross-sections through the density of non-condensed atoms in momentum space $n_{nc}(\mathbf{k}) = \langle \hat{\delta}^\dagger(\mathbf{k}) \hat{\delta}(\mathbf{k}) \rangle$ in the $k_x = 0$ plane after the end of the collision, for the bose enhanced case of $\alpha = 27.6$, $\beta = 31.6$. The labels A, B, C, D correspond to the four models introduced in the text. Color scale varies between plots. The black circle shows $|\mathbf{k}| = k_0$ for reference. The red (white) contour is at 0.1 (10^{-5}) of the peak condensate density.

models described below. The shorthand below names the kind of treatment for the condensate and non-condensate followed by the relevant equations

A full GP equation (2) + full Bogoliubov (8)

B SM (13) + full Bogoliubov (8)

C SM (13) + PP (12) equation \rightarrow what we call the RBM

D full GP equation (in the form (10)) + PP (12) equation.

In the following section we compare the distributions of scattered atoms obtained using the four above models.

3 Results

3.1 The shape of the halo

We first investigate the dynamics of the system in two characteristic cases, varying only α , while $\beta = 31.6$ is kept constant. It has been previously shown, that for Gaussian colliding clouds, significant Bose enhancement of scattering occurs when $\alpha^{(\text{past})}/\beta \approx 2$ or greater, i.e. $\alpha \gtrsim \beta$. Figures 1 and 2 show the cross-section through the halo of scattered atoms in the $k_x = 0$ plane at the end of the collision, for the case of appreciable ($\alpha = 27.6$) and negligible ($\alpha = 9.2$) bosonic enhancement of scattering. Density profiles of the halo in these two cases are shown in Figure 3.

When the dynamics of the $\hat{\delta}$ field is described by the simplified models C and D, the density of scattered atoms is spherically symmetric. On the other hand, this symmetry is lost within models A and B, where the halo of atoms is weakened near the condensates. This effect is due to the Bogliubov mean field (11b) and “off-resonant pairing” terms (11d). Notice that for larger interaction

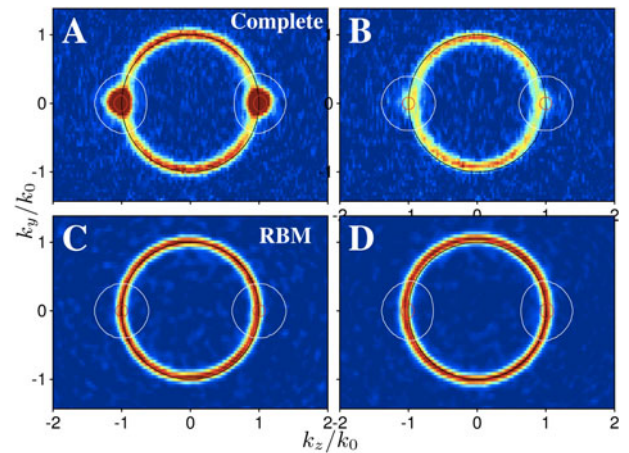


Fig. 2. (Color online) As Figure 1, but for the case of $\alpha = 9.2$, $\beta = 31.6$ where bosonic stimulation of scattering is negligible.

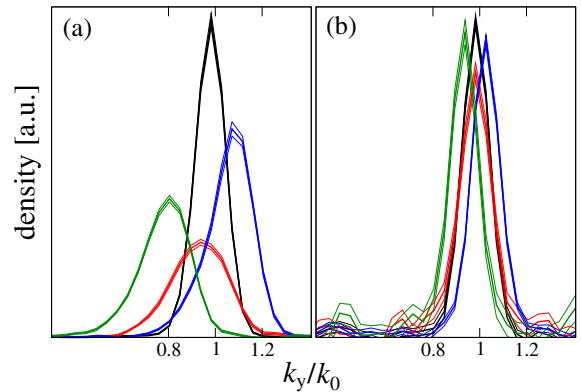


Fig. 3. (Color online) Cross-sections through the halo of scattered atoms along the k_y axis after the end of the collision for $\alpha = 27.6$ (a) and $\alpha = 9.2$ (b). The curves are calculated using the models A (red), B (green), C (black) and D (blue). Triple lines indicate the best statistical estimate and the $\pm 1\sigma$ statistical uncertainties in the mean.

strength – and consequently larger α – these phenomena are more pronounced. Moreover, models A and B predict some non-condensed atoms appearing on top of the BECs (in the same location as the BECs). The latter effect results from the term (11d) only.

3.2 Halo radius

In momentum space we denote the location of the maximum of the halo density by k_{max} . This quantity, discussed also in [1], varies between models A–D, as can be seen in Figures 1–3 in more detail. A shift of the position of the halo is obtained from an energy conservation argument when the BECs are modelled with two counter-propagating plane-waves [1,51]. The energy of a particle released from the condensates depends on the form of the GP equation we use to describe it. The full GP equation, with n – the mean density of the system, gives $\hbar^2 k_0^2/2m + \frac{3}{2}gn$, while the SM (13) gives a purely kinetic value $\hbar^2 k_0^2/2m$. On the other hand the energy needed to

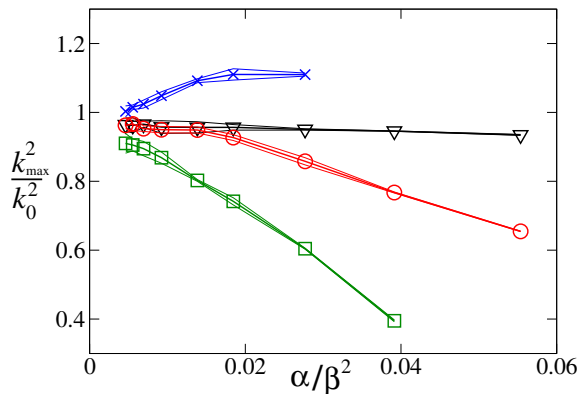


Fig. 4. (Color online) Dependence of the halo peak position k_{\max} on α/β^2 , calculated with A (red circles), B (green squares), C (black triangles) and D (blue \times). Error bars indicate the $\pm 1\sigma$ statistical uncertainties in the mean.

place a particle in a noncondensed mode with momentum $\hbar k$ is equal to $\hbar^2 k^2/2m + 2gn$ in the case of full Bogoliubov and $\hbar^2 k^2/2m$ in the case of the PP equation (12). Hence, using energy conservation we obtain

$$\begin{aligned} \text{A} \quad & \frac{\hbar^2 k^2}{2m} = \frac{\hbar^2 k_0^2}{2m} - \frac{1}{2}gn \\ \text{B} \quad & \frac{\hbar^2 k^2}{2m} = \frac{\hbar^2 k_0^2}{2m} - 2gn \\ \text{C} \quad & \frac{\hbar^2 k^2}{2m} = \frac{\hbar^2 k_0^2}{2m} \\ \text{D} \quad & \frac{\hbar^2 k^2}{2m} = \frac{\hbar^2 k_0^2}{2m} + \frac{3}{2}gn. \end{aligned}$$

This simplified model gives quite good agreement with the results presented in Figure 3.

Notice that in all models $(k/k_0)^2$ is a linear function of the parameter $gn \frac{2m}{\hbar^2 k_0^2}$. Recalling the definitions of α and β , we obtain a shift proportional to α/β^2 . To verify this conjecture, in Figure 4 we plot $(k_{\max}/k_0)^2$ as a function of α/β^2 for all four models. We observe that for growing α/β^2 (and thus growing α , as we keep constant $\beta = 31.6$), there is some deviation from the linear behaviour for models A and D. What these two models have in common is the full evolution of the condensates, which might make the picture of plane wave collisions with a time-independent density difficult to uphold. We also find that the linear model is in quite good agreement with the numeric results of Figure 4 if we take n to be half of the maximal density in the Thomas-Fermi approximation: $n = n_{\max}/2$, where $n_{\max} = (15/8\pi)N/R_{TF}^3$ (the factor of a half is arbitrary).

The “skiing effect” [1,52] should also be mentioned: Scattered atoms do not move freely after the initial pair creation, but roll-off the mean-field potential provided by the condensate (in models A and B). In this way, they recover part of the velocity lost when transferring from the condensate to the scattered field. This effect is probably a major contributor to the flattening out of the plots for model A and B at small α/β^2 in Figure 4.

Overall, for large interaction parameters α , the primary source of deviation for the simplified methods (B–D) from the physical result (A-red) is an incorrect

treatment of the mean field felt by the scattered atoms. Model D also deviates very strongly for large α values (data not shown) because the tails of the condensate broaden near the end of the collision and produce a bogus stimulated scattering for this model.

Finally, we note that for small enough α , the discrepancy between the RBM and full Bogoliubov treatment is negligible, as expected. The region of agreement ($\alpha \lesssim \beta$) matches approximately the region where stimulated scattering (Bose enhancement) is absent, although investigation with various values of β would be necessary to confirm or refute a link.

4 Conclusions

We have carried out a systematic analysis of the impact of the terms that are neglected in the simple RBM, often used to describe BEC collisions. It turns out that for interaction parameters α above a certain level, these terms are in fact crucial, and can qualitatively change the behaviour. The stochastic Bogoliubov method that we employ is a convenient tool for identifying the effect of the various physical processes. By taking apart the dynamics piece by piece, the processes responsible for the shift of the halo radius were identified (the mean field terms for the condensate and scattered atoms), as well as those which lead to the depletion of the halo along the collision axis (the mean field and off-resonant pairing terms (11d) for the Bogoliubov field).

The RBM model is still quantitatively correct when the interaction strength, as quantified by α , is sufficiently small.

We acknowledge fruitful discussions with C. Westbrook, D. Boiron and K. Kheruntsyan. M. T. acknowledges the support of Polish Government Research Grants for 2007-2011, P. D. for 2010–2013 and by the EU contract PERG06-GA-2009-256291. J. C. was supported by Foundation for Polish Science International TEAM Programme co-financed by the EU European Regional Development Fund.

References

1. V. Krachmalnicoff, J.-C. Jaskula, M. Bonneau, V. Leung, G.B. Partridge, D. Boiron, C.I. Westbrook, P. Deuar, P. Ziń, M. Trippenbach, K.V. Kheruntsyan, Phys. Rev. Lett. **104**, 150402 (2010)
2. J.-C. Jaskula, M. Bonneau, G.B. Partridge, V. Krachmalnicoff, P. Deuar, K.V. Kheruntsyan, A. Aspect, D. Boiron, C.I. Westbrook, Phys. Rev. Lett. **105**, 190402 (2010)
3. A.P. Chikkatur, A. Gorlitz, D.M. Stamper-Kurn, S. Inouye, S. Gupta, W. Ketterle, Phys. Rev. Lett. **85**, 483 (2000)
4. J. Steinhauer, R. Ozeri, N. Katz, N. Davidson, Phys. Rev. Lett. **88**, 120407 (2002)
5. N. Katz, J. Steinhauer, R. Ozeri, N. Davidson, Phys. Rev. Lett. **89**, 220401 (2002)

6. J.M. Vogels, K. Xu, W. Ketterle, Phys. Rev. Lett. **89**, 020401 (2002)
7. A. Perrin, C.M. Savage, D. Boiron, V. Krachmalnicoff, C.I. Westbrook, K.V. Kheruntsyan, New J. Phys. **10**, 045021 (2008)
8. J.M. Vogels, J.K. Chin, W. Ketterle, Phys. Rev. Lett. **90**, 030403 (2003)
9. N. Katz, R. Ozeri, E. Rowen, E. Gershnel, N. Davidson, Phys. Rev. A **70**, 033615 (2004)
10. C. Buggle, J. Leonard, W. von Klitzing, J.T.M. Walraven, Phys. Rev. Lett. **93**, 173202 (2004)
11. N. Katz, E. Rowen, R. Ozeri, N. Davidson, Phys. Rev. Lett. **95**, 220403 (2005)
12. A. Perrin, H. Chang, V. Krachmalnicoff, M. Schellekens, D. Boiron, A. Aspect, C.I. Westbrook, Phys. Rev. Lett. **99**, 150405 (2007)
13. R.G. Dall, L.J. Byron, A.G. Truscott, G.R. Dennis, M.T. Johnson, J.J. Hope, Phys. Rev. A **79**, 011601(R) (2009)
14. M. Kozuma, L. Deng, E.W. Hagley, J. Wen, R. Lutwak, K. Helmerson, S.L. Rolston, W.D. Phillips, Phys. Rev. Lett. **82**, 871 (1999)
15. L. Deng, E.W. Hagley, J. Wen, M. Trippenbach, Y. Band, P.S. Julienne, J.E. Simsarian, K. Helmerson, S.L. Rolston, W.D. Phillips, Nature **398**, 218 (1999)
16. P. Maddaloni, M. Modugno, C. Fort, F. Minardi, M. Inguscio, Phys. Rev. Lett. **85**, 2413 (2000)
17. Y.B. Band, J.P. Burke Jr., A. Simoni, P.S. Julienne, Phys. Rev. A **64**, 023607 (2001)
18. Y.B. Band, M. Trippenbach, J.P. Burke, P.S. Julienne, Phys. Rev. Lett. **84**, 5462 (2000)
19. M. Trippenbach, Y.B. Band, P.S. Julienne, Phys. Rev. A **62**, 023608 (2000)
20. V.A. Yurovsky, Phys. Rev. A **65**, 033605 (2002)
21. R. Bach, M. Trippenbach, K. Rzazewski, Phys. Rev. A **65**, 063605 (2002)
22. J. Chwedenczuk, M. Trippenbach, K. Rzazewski, J. Phys. B **37**, L391 (2004)
23. K. Molmer, A. Perrin, V. Krachmalnicoff, V. Leung, D. Boiron, A. Aspect, C.I. Westbrook, Phys. Rev. A **77**, 033601 (2008)
24. A.A. Norrie, R.J. Ballagh, C.W. Gardiner, Phys. Rev. Lett. **94**, 040401 (2005)
25. P. Zin, J. Chwedenczuk, A. Veitia, K. Rzazewski, M. Trippenbach, Phys. Rev. Lett. **94**, 200401 (2005)
26. P. Zin, J. Chwedenczuk, M. Trippenbach, Phys. Rev. A **73**, 033602 (2006)
27. A.A. Norrie, R.J. Ballagh, C.W. Gardiner, Phys. Rev. A **73**, 043617 (2006)
28. J. Chwedenczuk, P. Zin, K. Rzazewski, M. Trippenbach, Phys. Rev. Lett. **97**, 170404 (2006)
29. P. Deuar, P.D. Drummond, Phys. Rev. Lett. **98**, 120402 (2007)
30. P.D. Drummond, P. Deuar, J.F. Corney, Opt. Spectrosc. **103**, 7 (2007)
31. J. Chwedenczuk, P. Zin, M. Trippenbach, A. Perrin, V. Leung, D. Boiron, C.I. Westbrook, Phys. Rev. A **78**, 053605 (2008)
32. M. Ogren, K.V. Kheruntsyan, Phys. Rev. A **79**, 021606(R) (2009)
33. P. Deuar, Phys. Rev. Lett. **103**, 130402 (2009)
34. Y. Wang, J.P. D'Incao, H.-C. Nagerl, B.D. Esry, Phys. Rev. Lett. **104**, 113201 (2010)
35. P.G. Kwiat, K. Mattle, H. Weinfurter, A. Zeilinger, A.V. Sergienko, Y. Shih, Phys. Rev. Lett. **75**, 4337 (1995)
36. N. Gisin, G. Ribordy, W. Tittel, H. Zbinden, Rev. Mod. Phys. **74**, 145 (1998)
37. D. Bouwmeester, J.-W. Pan, K. Mattle, M. Eibl, H. Weinfurter, A. Zeilinger, Nature **390**, 575 (1997)
38. H.A. Bachor, T.C. Ralph, *A guide to experiments in quantum optics*, 2nd edn. (Wiley-VCH, Berlin, 2004)
39. C. Gross, T. Zibold, E. Nicklas, J. Esteve, M.K. Oberthaler, Nature **464**, 1165 (2010)
40. P. Bouyer, M. Kasevich, Phys. Rev. A **56**, R1083 (1997)
41. J.A. Dunningham, K. Burnett, S.M. Barnett, Phys. Rev. Lett. **89**, 150401 (2002)
42. R.A. Campos, C.C. Gerry, A. Bennoussa, Phys. Rev. A **68**, 023810 (2003)
43. M.D. Reid, P.D. Drummond, W.P. Bowen, E.G. Cavalcanti, P.H. Lam, H.A. Bachor, U.L. Andersen, G. Leuchs, Rev. Mod. Phys. **81**, 1727 (2009)
44. F. Dalfvo, S. Giorgini, L.P. Pitaevskii, S. Stringari, Rev. Mod. Phys. **71**, 463 (1999)
45. C.W. Gardiner, P. Zoller, *Quantum Noise* (Springer, New York, 2004)
46. C.W. Gardiner, *Handbook of Stochastic Methods* (Springer, Berlin, New York, 1983)
47. P.D. Drummond, C.W. Gardiner, J. Phys. A **13**, 2353 (1980)
48. P. Deuar, Ph.D. thesis, [arXiv:cond-mat/0507023](https://arxiv.org/abs/cond-mat/0507023)
49. P. Deuar, J. Chwedenczuk, M. Trippenbach, P. Ziń, Phys. Rev. A, in press
50. P. Deuar, P.D. Drummond, Phys. Rev. A **66**, 033812 (2002)
51. P. Szańkowski, P. Ziń, M. Trippenbach, unpublished
52. K.V. Kheruntsyan, private communication